16th World Conference on Earthquake, 16WCEE 2017
Santiago Chile, January 9th to 13th 2017
Paper N° 4500
Registration Code: S-XXXXXXXX

Evaluation of seismic response of large land based wind turbines in the near-fault area using different analysis methods

G.Ö. Sigurðsson(1), R. Rupakhety(2), S. Ólafsson(3)

(1) *Research Scientist, Earthquake Engineering Research Centre, University of Iceland, gos12@hi.is*
(2) *Professor, Earthquake Engineering Research Centre, University of Iceland, rajesh@hi.is*
(3) *Research Professor, Earthquake Engineering Research Centre, University of Iceland, simon@hi.is*

Abstract

The dynamic response of a 5-MW land based wind turbine is calculated using different analysis methods. These methods include time history analysis using a large number of recorded near-fault ground motions; response spectral analysis using spectral shapes recommended in design codes; and that using near-fault specific response spectral model. The turbine tower is modelled with three dimensional beam-column elements with head masses lumped at the top of the tower. Results from linear elastic time series simulation indicate that overturning moment demand for a range of earthquake magnitude may exceed that due to extreme wind loads, making seismic loading in the near field a design-driving factor. It is found that the dominant period of near-fault ground motion relative to the fundamental structural period is a critical factor controlling seismic response. The results indicate that Eurocode 8 spectral shapes, even when scaled by peak ground acceleration of recorded near-fault ground motions, are not suitable to simulate seismic response of wind turbines. The response simulated using a near-fault specific response spectral model [1, 2] shows good correlation with those obtained from time history analysis.

Keywords: Wind turbine, response spectra, near-fault ground motion, pulse period

1. Introduction

The wind turbine structure being used in this study is the one described by [3]. The turbine is a conventional three-bladed upwind variable-speed type. The main focus of the study is on the tower structure; the modelling of the nacelle and rotor are simplified as rigid masses. The base or the foundation of the tower is considered as rigidly fixed, assuming that the structure is land based and set up on a rock site. The tower itself is a steel circular hollow-section with a diameter and thickness which decreases along the height. A finite element model of the tower is created by using linear elastic beam-column elements (100 elements in the tower). The diameter and the thickness of the tower are assumed to reduce linearly from the base to the top of the tower. The thickness of the tower wall is increased by 30% throughout the height of the tower to account for flanges, bolts, etc. The flexibility of nacelle and rotor is not considered; however, their inertia is modelled by lumped head mass applied at the top of the tower. The damping ratio used is 1% of critical damping, which is the recommended value used in most standards [4]. The translational and rotational head mass applied at the tip are listed in Table 1 along with other relevant parameters of the model.

The modal properties obtained from Eigen value analysis are compared to those reported in the published literature. Seismic response corresponding to a large number of recorded near-fault ground motions is evaluated by using time history analysis as well response spectral analysis methods. The ground motions being considered are near-fault ground motions, containing strong velocity pulses.

Table 1– Properties of the wind turbine used in this study (based on [5]).

Property	**Value**
Rating	5 MW
Tower Height	87.6 m
Base, Top Diameter	6.00 m, 3.87 m
Base, Top shell thickness	27 mm, 19 mm
Elastic modulus	210 GPa
Rotor Mass	110,000 kg
Nacelle Mass	240,000 kg
Tower Mass	347,460 kg
Tower Head moment of inertia about rotor-parallel axis (x direction)	4.37×10^7 kgm^2
Tower Head moment of inertia about lateral axis	2.35×10^7 kgm^2
Tower Head moment of inertia about vertical axis	2.54×10^7 kgm^2

2. Modal analysis

Undamped natural frequencies obtained from eigenvalue analysis of the finite element model are presented in Table 2 for side-to-side (SS) and for-aft (FA) motion, with the effective modal mass along the perpendicular directions computed separately. For comparison, the frequencies reported by Bir and Jonkman [5] using BModes and ADAMS software are also presented. The significant modes participating in perpendicular directions are highlighted. As seen in Table 2 the effective modal mass is nearly the same in both directions, and the 4 first modes account for more than 90% of effective modal mass in both cases.

The normalized mode shapes of the tower are presented schematically in Fig. 1. As can be seen from Fig. 1, the mode shapes in SS and FA directions are nearly identical. Due to the similarity of the directions they can be regarded as having the same response—in parked state—in the two directions, therefore it is sufficient to analyze seismic response in one of the two direction. The for-aft motion (parallel to the rotor axis) is subsequently studied since the first mode has a slightly higher participation in for-aft than in side-to-side direction. The earthquake excitation is applied unidirectional in the for-aft direction.

3. Time history analysis

The near-fault ground motion data used in this study is a subset of data described in [1, 2]. The strong ground motion data are collected from 29 different earthquake events, mostly from the Next Generation Attenuation (NGA) database. Strong-motion records from the June 2000 Earthquakes and May 2008 Earthquake in South-Iceland were obtained from the Internet Site for Strong Motion Data (ISESD). Records from the Parkfield Earthquake are obtained from the California Integrated Seismic Network (CISN). Records from soft sites (average shear wave velocity in the upper 30 m less than 260) are excluded. Moreover, only records within 30 km distance from the causative faults are considered. Further details in the selection of ground motion records is given in [Sigurðsson 2015]. A total of 70 ground motions which range from 5.7 to 7.6 in moment magnitude are used for the analysis. The structural damping ratio is assumed to be 1% in all the modes and Newmark's integration scheme [6] is used.

Table 1 – The modal properties of the 5MW wind turbine tower, the highlighted lines mark the modes contributing to seismic response in SS motion [5].

Mode number	Mode type	Frequency (Hz)			Effective modal mass
		This study	BModes	ADAMS	
1	1st SS	0.328	0.329	0.319	67.6%
2	1st FA	0.332	0.332	0.322	69.4%
3	1st Torsional	1.478	1.470	1.476	0.0%
4	2nd SS	1.801	1.880	1.882	10.6%
5	2nd FA	2.278	2.243	2.239	10.7%
6	3rd SS	4.583	4.652	4.724	8.1%
7	3rd FA	5.056	4.986	5.183	6.3%
8	1st Axial	7.927	8.131	7.937	0.0%
9	4th SS	11.27	11.31	11.268	4.2%
10	4th FA	11.43	11.45	11.472	4.1%

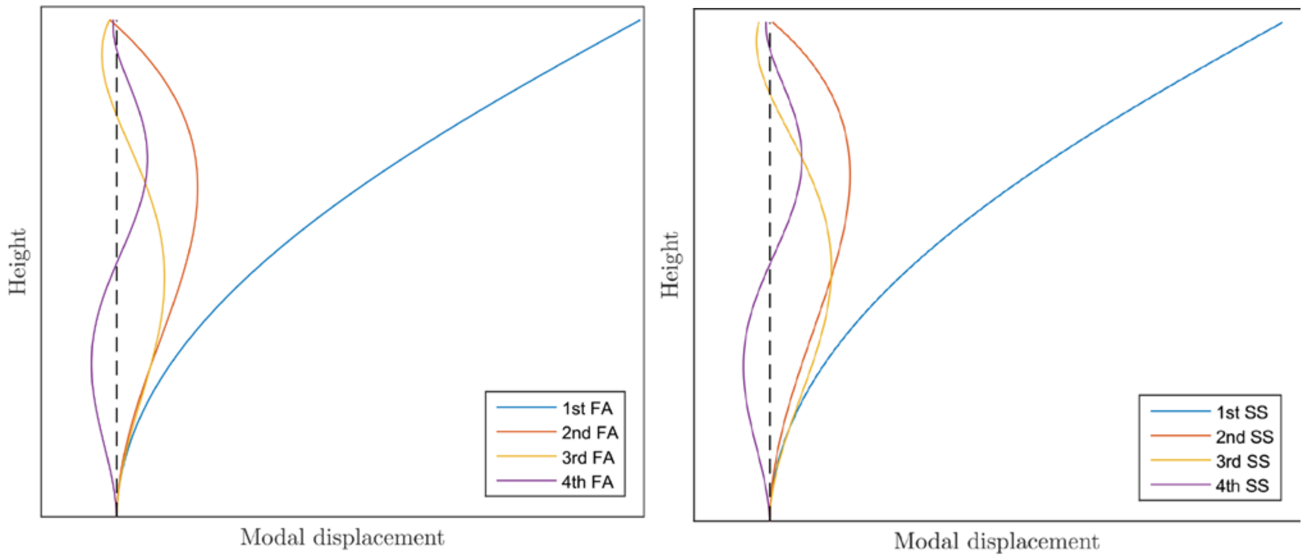

Fig. 1 – The first few mode shapes of a) for-aft motion and b) side-to-side motion

4. Response spectra analysis

For the response spectral analysis, a choice of an adequate response spectra must be made for any given site. The standard practice in Europe is to use the EC8 response spectra [7] to obtain the design load from earthquake events. For a site close to earthquake faults, forward directivity effects result in pulse-like ground motions whose spectral shapes are different from those recommended in the EC8. The effect of such motions is considered in this study by using the response spectral shape proposed by [1]. This model is hereafter referred to as the RR2011 model. The spectral shapes from EC8 are scaled by the peak ground acceleration of the recorded ground motions in order to make a valid comparison with the response computed from time history analysis. Modal combination is based on the square root of the sum of the squares (SRSS) rule.

Spectral shapes corresponding to the RR2011 model for 5% of critical damping are shown in Fig. 2 for different earthquake magnitude. These spectral shapes represent pseudo-spectral velocity (PSV) normalized by the peak ground velocity (PGV). These shapes are scaled with the PGV of the recorded ground motions used in time history analysis and the resulting PSV are converted to PSA. Response spectral analysis using EC8 spectral shapes and SRSS combination rule is hereafter called as EC8 SRSS, and it is called as RR2011 SRSS when the RR2011 model is used. Response is also evaluation by using SRSS-based response spectral method using the actual response spectra of each ground motion. This method of analysis is hereafter called as GM SRSS.

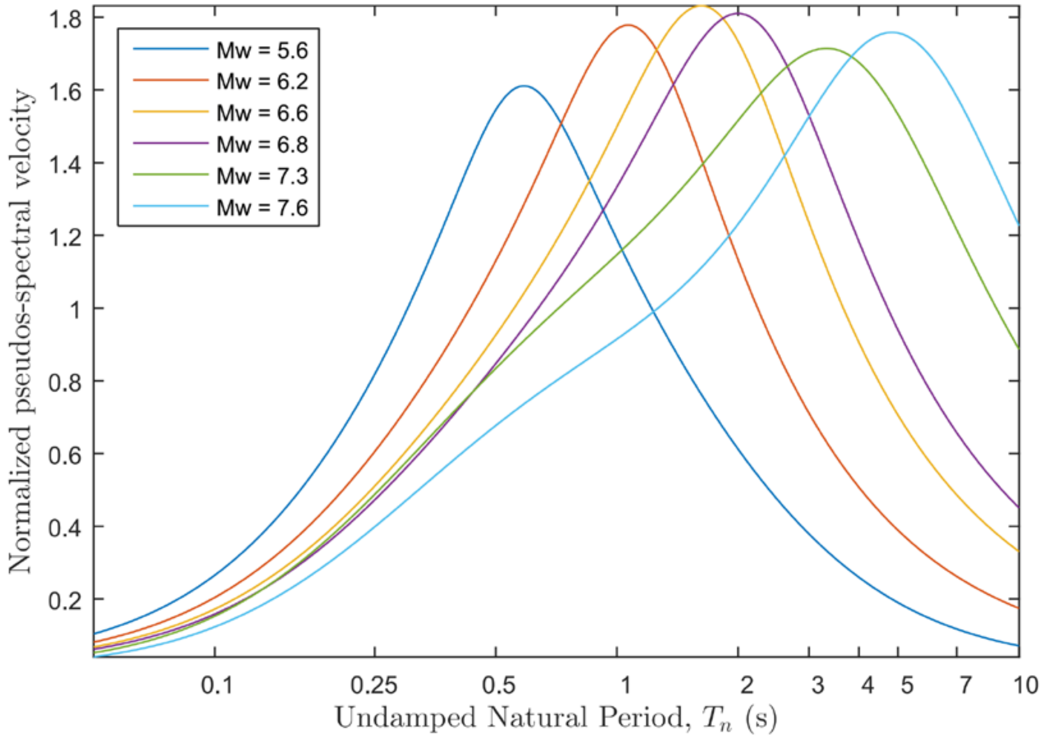

Fig. 2 – Normalized pseudo-spectral velocity (PSV_n) for different earthquake magnitudes.

5. Displacement response

Maximum horizontal displacements of the nacelle obtained from time history analysis using 70 near-fault ground motions are shown in Fig. 3 as a function of the normalized pulse period of ground motion (pulse period over the fundamental structural period). The average value of maximum displacement is roughly 0.5 meters with values ranging between a few centimetres to 1.5 m. As is evident from Fig. 3, the maximum displacement caused by ground motions with a pulse period near the fundamental structural period are significantly larger than others. These is caused by the resonant behaviour of the structure to the dominant pulse contained in the ground motion. It is interesting to note that some of the earthquakes with smaller magnitude produce a larger response than those with larger magnitude. The main reason behind this is the scaling of pulse period with earthquake size. For this specific type of structure, the fundamental period of vibration is close to the pulse periods of earthquakes in the magnitude range 6.5-6.9, and therefore earthquakes of this size are the most critical.

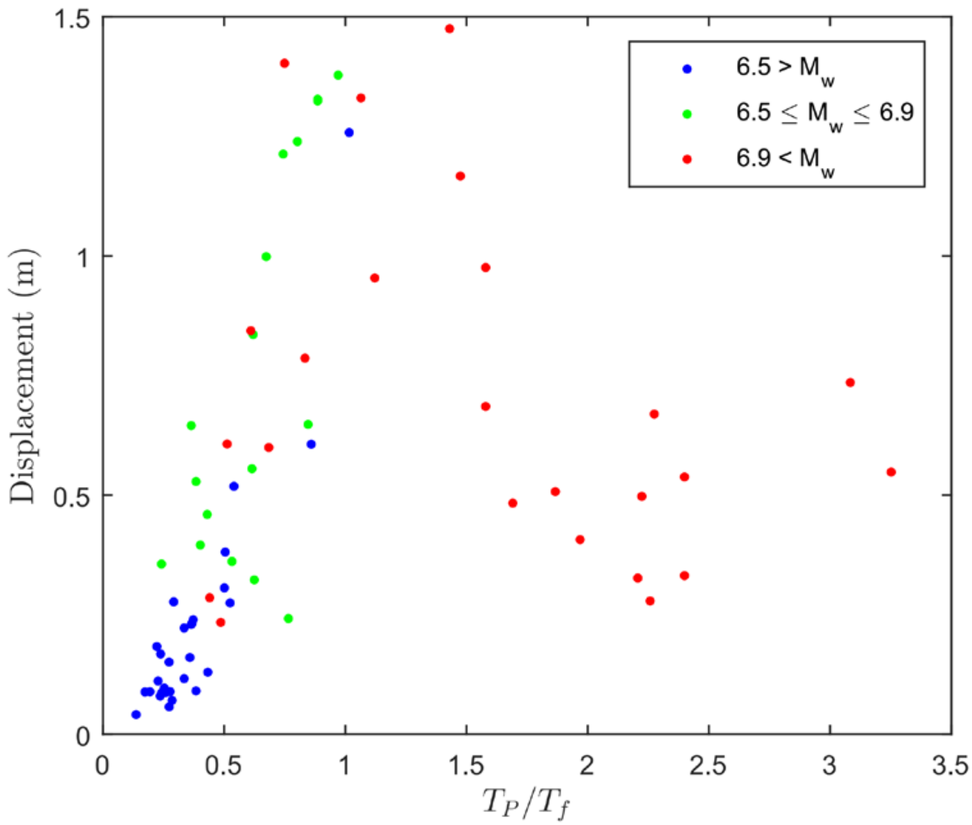

Fig. 3 – Maximum horizontal nacelle displacement due to 70 near-fault ground motions; the results are divided into different magnitude bins as indicated in the legend. The horizontal axis represents the predominant period of velocity pulse [1] normalized by the fundamental period of vibration of the structure.

Average maximum displacement demands at the top of the tower for each magnitude bin are shown in Fig. 4 for the four analysis procedures described previously. It is evident that the two larger bins produce significantly larger displacement demands than the bin with smaller earthquakes. Time history and GM SRSS results are very close to each other, implying that response spectral analysis is appropriate as long as the spectrum used in analysis is accurate. RR2011 results for average displacement in each bin, seem to adequately simulate the response of the structure. EC8 spectral shapes, even when scaled with the PGA of individual ground motion, seem to over-estimate the response for small magnitude earthquakes, and significantly under-estimate it for larger earthquakes. This is not surprising considering that EC8 spectral shape is based mostly on far-fault ground motion records, and fail to account for near-fault pulses.

The average drift ratio (across all ground motions), which may be considered the slope of the deformed tower along its height, is shown in Fig 5 (a). The contributions of the first three modes of vibration are also shown. The drift demand is the largest for the second bin. This is due to the proximity of pulse period to the fundamental structural period (see Fig. 3).

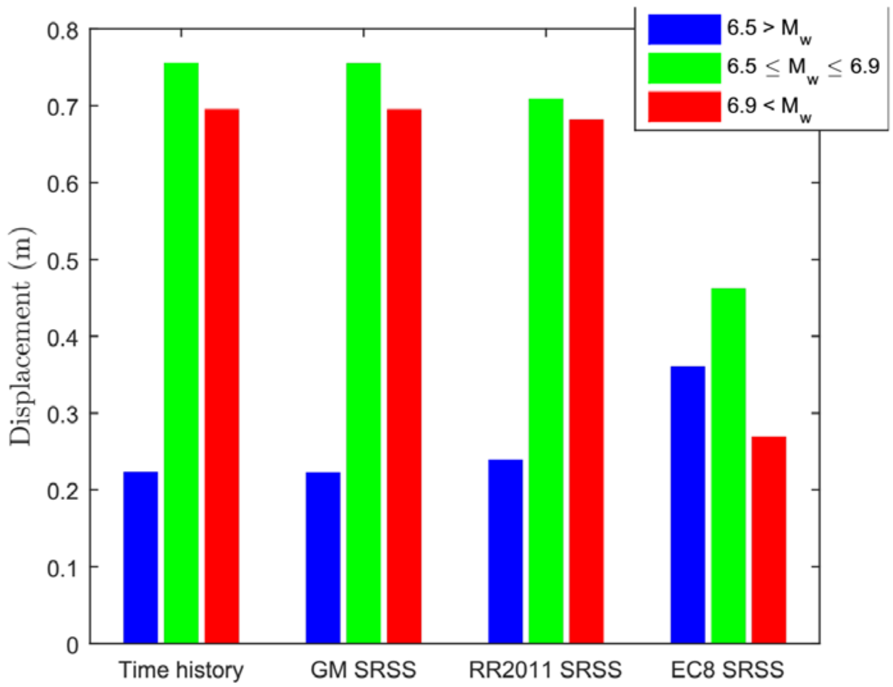

Fig. 4 – Average maximum nacelle displacement in three different magnitude bins computed from time history and response spectral analysis procedures.

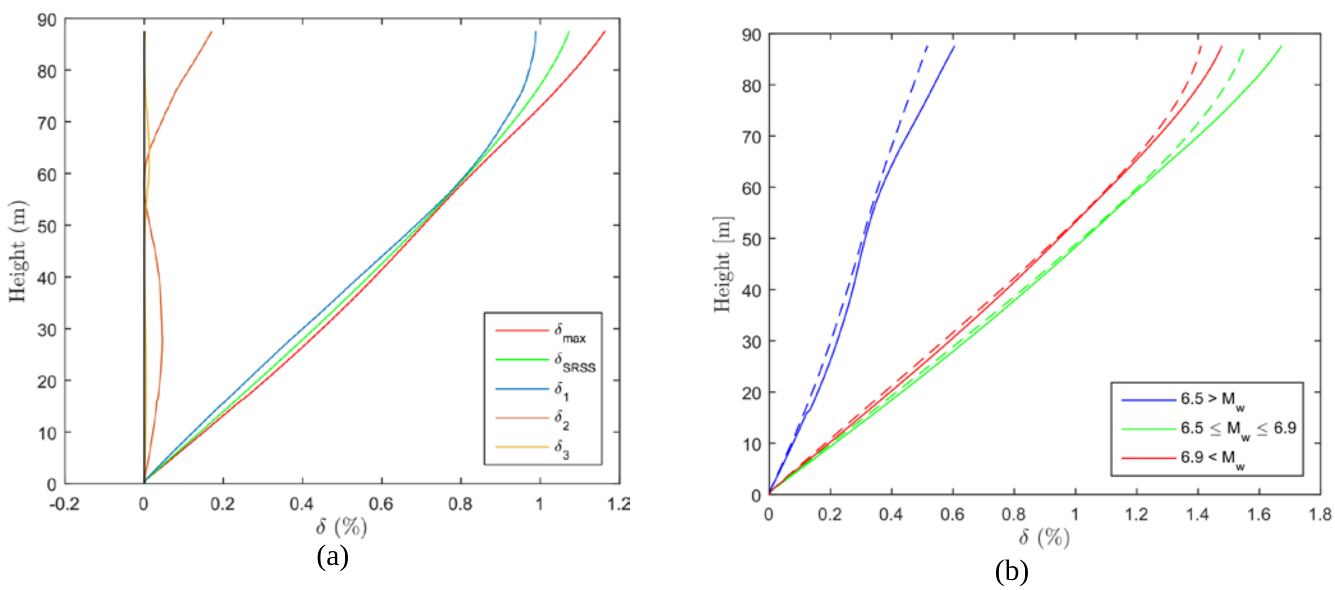

Fig. 5 – (a) Average (for all the ground motions) drift ratio along the height of the tower. The red curve corresponds to the time history results, the green curve to GM SRSS, and the other curves represent contribution of the first three significant modes of vibration as indicated in the legend. (b) Average drift ratio of all the motions using time-history (solid) and response spectra method (dashed) classified into three magnitude bins.

5. Base shear and overturning moment demand

The base shear demand of the structure due to all the ground motions is shown in Fig. 5 (a). As with the displacement response, there is a clear amplification of base shear when the pulse period is close to the fundamental period of the structure, although in this case, there appears to be a significant increase in the variance of the values. The results indicate that the base shear demand is the largest when the pulse period to structural period ratio is in the range 0.5-1.5. The sharp amplification of response near resonance is also due to the fact that the damping ratio of the tower is rather small. Providing supplemental damping to the structure can significantly reduce this resonance effect. It is noteworthy how larger magnitude earthquakes appear to produce, on the average, lower base shear demands than smaller ones. This is due to the fact that as earthquake size increases, the dominant period of ground motion increases, with more energy being radiated at longer periods, and less energy at high frequencies. Since base shear is related to peak acceleration response, it is subsequently sensitive to high frequency content of ground motion, larger earthquakes seem to produce relatively lower PSA (but higher PSV and SD) and therefore lower base shear demand.

Similar results regarding overturning moment demands are shown in Fig. 6b. The maximum overturning moment is around 325 MNm. These demands exceed moment demands due to extreme wind loads, based on extensive simulations [8, 9]. Another study [10] reported a maximum overturning moment demand of 153 MNm which is also considerably smaller than that due to near-fault seismic loads considered here.

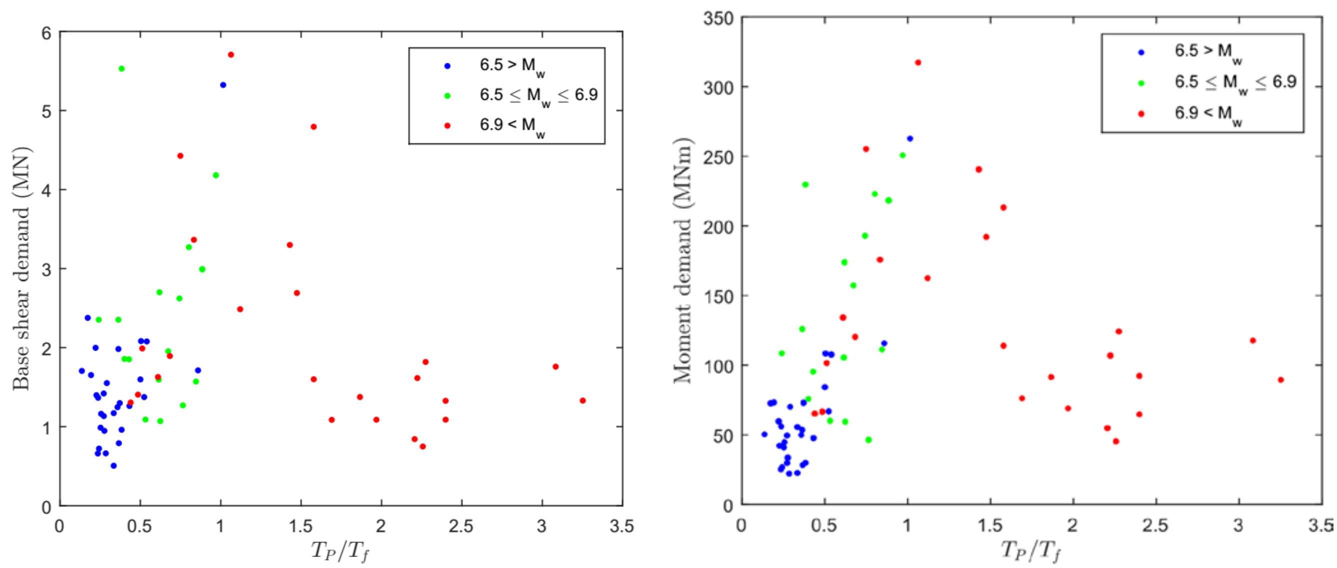

(a) (b)

Fig. 6 – (a) Base shear demand due to each ground motion; the results are divided into different magnitude bins as indicated in the legend. (b) Same as is (a) but for overturning moment demand

The average base shear and overturning moment demands in different magnitude bins obtained from the four analysis methods are compared in Fig. 6 As for displacement demands, moderate to large earthquakes (magnitude in the range 6.5 to 6.9) produce the largest demands in the structure. Very large earthquakes produce smaller demands than the moderate to large earthquakes as the pulse period in these earthquakes is larger than the fundamental period of the structure being considered. Unlike displacement demand, average response obtained from response spectral analysis and the actual response spectra are significantly different, the latter being slightly lower. The response predicted by the RR2011 response spectral models are as good as those obtained from the actual response spectra of the ground motions, which indicates that the RR2011 model is a good representative of average spectral contents of near-fault ground motions. The EC8 spectral shapes are found to under-estimate the response due to moderate to large and very large earthquakes and over-estimate that due to small to moderate earthquakes.

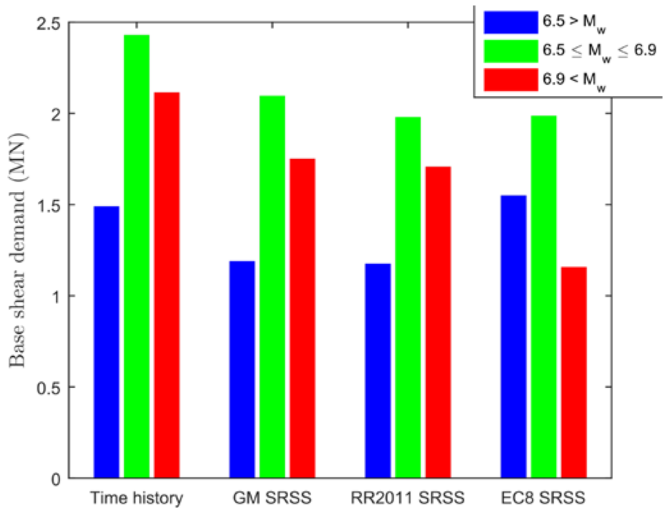

(a)

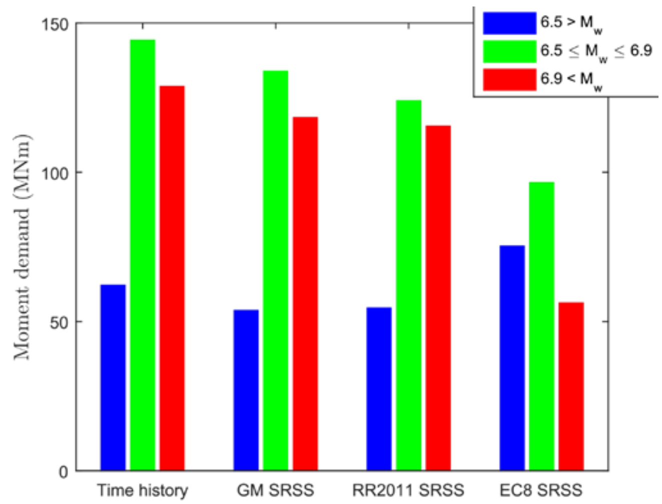

(b)

Fig. 7 – (a) Average base shear demand in different magnitude bins (b) Average overturning moment demand in different magnitude bins

5. Discussion and conclusions

To explain the differences in the results obtained from different analysis methods, reference is made to Fig. 8. The EC8 spectrum significantly under-estimates the average spectral acceleration of the second bin (moment magnitude in the range 6.5-6.9) at the fundamental structural period. This results in under-estimation of response. It is noted that although the EC8 spectrum over-estimates spectral acceleration at higher modes, and yet, results in under-estimation of moment demand. This is due to smaller mass participation in higher modes of vibration. The same conclusions apply to very large earthquakes. For small to moderate earthquake (moment magnitude less than 6.5), the EC8 spectral acceleration at the fundamental period of the structure is slightly above the average spectral shape of recorded ground motions. This results in over-estimation of structural response. The spectral model proposed by [1] captures the average spectral shapes of recorded motion adequately and therefore the results obtained from this model are as good as those obtained from the actual response spectra of the recorded ground motions.

The results indicate that the EC8 model is not suitable to evaluate seismic action on tall wind turbine towers in the near-fault area. This is due to the inability of the model to account for long-period energy content of ground motions forward directivity region near earthquakes fault. The RR2011 model was found, on the average, to represent the results obtained from time history analysis very well. It is observed that response spectral analysis using the SRSS combination rule gives satisfactory results as long as a proper response spectrum is used. Higher mode effects are found to be significant at the top of the tower. As almost the half of the total mass is located at the top of the tower, higher mode effects are seen to be significant in base shear and overturning moment. Displacement demand, however, is seen to be less sensitive to higher modes. The results indicate that earthquake loads may indeed be design-driving for large wind turbines and particularly in areas that are in the near-fault region. The results also indicate that the most critical ground motions for the wind turbines of this type are near-fault earthquakes with moment magnitude in the range 6.5 to 6.9. This is mainly due to the fact that in this magnitude range, the pulse period is close to the fundamental period of the structure. It seems that seismic loads due to near-fault ground motions are the largest when the pulse period is between about 0.5 to 1.5 times the fundamental period of the structure.

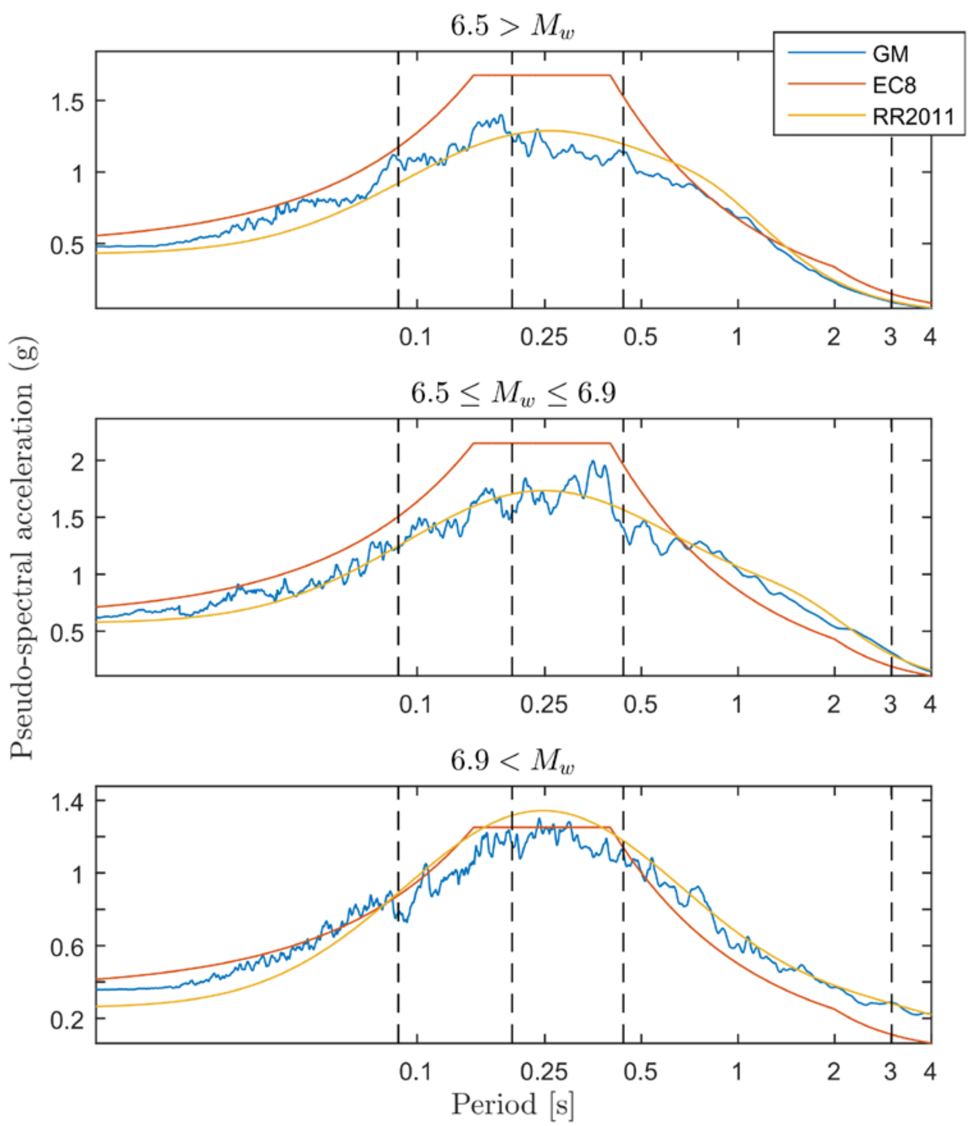

Fig. 8 – The average response spectra of each bin plotted against the equivalent EC8 spectra.

6. Acknowledgements

GÖS acknowledges financial grants from Vísinda- og rannsóknarsjóður Suðurlands managed by Fræðslunet Símenntunar á Suðurlandi and Háskólafélag Suðurland and a project grant from Félagstofnun stúdenta. RR and SÓ acknowledge financial support from the University of Iceland research fund and the National Power Company of Iceland, Landsvirkjún.

7. References

[1] Rupakhety R, Sigurdsson SU, Papageorgiou AS, Sigbjörnsson R (2011): Quantification of ground-motion parameters and response spectra in the near-fault region. *Bulletin of Earthquake Engineering,* **9**:893-930.

[2] Rupakhety R, Sigbjörnsson R. (2011): Can simple pulses adequately represent near-fault ground motions? *Journal of Earthquake Engineering*,**15**(8), 1260-1272.

[3] Butterfield S, Musial W, Scott G (2009): Definition of a 5-MW reference wind turbine for offshore system development. National Renewable Energy Laboratory.

[4] Wind G. L. (2005): Guideline for the Certification of Offshore Wind Turbines. Germanischer Lloyd Industrial Services GmbH.

[5] Bir G, Jonkman J (2008): Modal dynamics of large wind turbines with different support structures. In *ASME 27th International Conference on Offshore Mechanics and Arctic Engineering*. American Society of Mechanical Engineers.

[6] Newmark NM (1959): A method of computation for structural dynamics. *Journal of the engineering mechanics division*, **85**(3):67-94.

[7] CEN (2004): Eurocode 8: Design of Structures for Earthquake Resistance—Part 1: General Rules. Seismic Actions and Rules for Buildings.

[8] Prowell I (2011) An Experimental and Numerical Study of Wind Turbine Seismic Behavior. PhD Thesis, University of California, San Diego.

[9] Fogle J, Agarwal P, Manuel L (2008): Towards an improved understanding of statistical extrapolation for wind turbine extreme loads. *Wind Energy*, **11**(6):613.

[10] Jonkman JM (2007): Dynamics modeling and loads analysis of an offshore floating wind turbine. ProQuest.